JOURNAL OF SPACECRAFT AND ROCKETS
Vol. 43, No. 2, March–April 2006

Two Thermodynamics-Based Approaches to Atomic Oxygen Sensing

Mikhail L. Zheludkevich* and Kiryl A. Yasakau†
University of Aveiro, 3810-193 Aveiro, Portugal
and
Anatoly G. Gusakov,‡ Anatoly G. Voropaev,§ and Alim A. Vecher¶
Belarusian State University, 220050, Minsk, Republic of Belarus

Impact of atomic oxygen is a main factor responsible for enhanced oxidation and fast degradation of spacecraft and satellite construction materials in low earth orbits. Thus, information concerning atomic oxygen concentration is important for spacecraft designers and manufacturers. Many sensors have been developed to perform atomic oxygen concentration measurement. However, these sensors have important disadvantages: high power consumption, low reproducibility, limited lifetime, and large mass/size parameters. In the present work two new methods based on a thermodynamic approach are proposed, employing an enhanced chemical potential of atomic oxygen. The first method is based on measurement of maximal temperature of silver oxidation in atomic oxygen, since this temperature depends on the concentration of oxygen in atmosphere. The second method is based on a Nernstian-type sensor with oxygen-conducting solid electrolyte. The electromotive force of this cell also depends on the concentration of atomic oxygen in the gas phase. Thermodynamic interpretations of sensor operation are proposed. The results of laboratory experiments on atomic oxygen pressure estimation by both methods are in good agreement. A new complex sensor using both approaches in one device is developed.

I. Introduction

THE surfaces of spacecraft and satellites located in low earth orbits are exposed to a substantial flux of oxygen atoms (ca. 10^{15} atoms $\cdot$ cm$^{-2} \cdot$ s^{-1}) (Ref. 1). Atomic oxygen has sufficiently higher oxidation ability than the diatomic gas to cause faster oxidative degradation of polymeric and metallic construction and functional materials.[2–7] For example, silver, which is a popular material for space applications due to its low electrical resistance and superior reflectivity in a wide optical range, is fast oxidized in low earth orbit. Therefore, information concerning the fluxes of atomic oxygen is very important for spacecraft designers to predict the lifetime of constructional and functional materials in contact with the space environment.

Many spectrometric, optical, gravimetric, and semiconductor-based methods for atomic-oxygen sensing have been developed.[1,8–12] Advantages as well as disadvantages of some most useful methods are reviewed in the following.

Mass spectrometers were used in several missions to measure the atomic oxygen concentration. However, large weight/size parameters and high energy consumption limit the use of this method.[1] ZnO-based semiconductor sensors have been developed for sensing atomic oxygen species.[10–12] The adsorbed oxygen atoms cause depletion of electron charge carriers, decreasing electrical resistance of *n*-type semiconductor (ZnO). However, these sensors show slow response even when produced as a thin film. Some methods use a high chemical potential and enhanced oxidation ability of the atomic oxygen for different materials.[8,9] Measurements of the material oxidation rate can provide information concerning the concentration of atomic oxygen. Kapton®, carbon, and silver are normally used as a working element in such sensors.[1,8,9] Thin films of these materials can be deposited on a quartz crystal microbalance that is very sensitive to weight changes. In the case of a silver sensing element, the rate of oxidation can be estimated by monitoring film resistance evolution due to decrease of its thickness during exposure to atomic oxygen fluxes.[9] Sensors based on materials degradation are not reusable. Moreover, kinetics of the heterogenous reactions depends on the film structure and the surface morphology. In the case of silver-based sensors, cracking and flaking of silver oxide can also sufficiently influence the oxidation kinetics.[1]

Two new methods based on a thermodynamic approach are proposed in the present work. The main idea of the methods is to transform the excess chemical potential of atomic oxygen to an electrical signal. In the first case the excess chemical potential is transformed to the energy of chemical reaction of silver oxidation, changing the temperature range of silver oxide formation. The chemical potential of atomic oxygen can also be directly transformed to electromotive force (EMF) of a Nernstian cell with an oxygen-conductive solid electrolyte.

Two sensors based on these ideas are developed in the present work and tested in an atomic oxygen atmosphere.

II. Experimental

A. Atomic Oxygen Generation

Experiments were performed using a high-vacuum setup described in detail elsewhere.[13] Sensors were placed in a vacuum chamber evacuated by a diffusion pump. A flux of air was introduced into the chamber and controlled by a needle valve. Atomic oxygen was generated by passing the air through a microwave discharge with frequency 2450 MHz and power 60 W. Typical value of degree of oxygen dissociation was 28%. The flux density of atomic oxygen was measured using the method of chemiluminescent titration with nitrogen dioxide. This method is based on interaction of oxygen atoms with NO_2 molecules, which produce luminescence according to the following reactions:

$$NO_2 + O \rightarrow NO + O_2, \qquad \text{fast reaction} \qquad (1)$$

$$NO + O \rightarrow NO_2 + h\nu, \qquad \text{slow reaction} \qquad (2)$$

Received 11 December 2004; revision received 17 August 2005; accepted for publication 10 September 2005.

*Postdoctoral Associate, Department of Ceramics and Glass Engineering.
†Ph.D. Student, Department of Ceramics and Glass Engineering.
‡Senior Researcher, Department of Chemistry, 14 Leningradskaya Street.
§Head of Laboratory, Department of Chemistry, 14 Leningradskaya Street. Deceased.
¶Full Professor, Department of Chemistry, 14 Leningradskaya Street.

Nitrogen dioxide reacts fast with oxygen atoms, producing nitrogen oxide and molecular oxygen. Nitrogen oxide, in turn, can also react with atomic oxygen, emitting a quantum of light. The latter reaction is slower than the former. Thus, oxygen atoms are completely consumed in reaction (1) without emission of light when there is no excess of atomic oxygen. However, the chemiluminescent reaction occurs when the concentration of NO_2 is lower than a stoichiometric concentration of atomic oxygen. Hence, the concentration of NO_2, when luminescence disappears, is a single-valued characteristic of the atomic oxygen concentration. The measured flux density of atomic oxygen in the experiments was about 2.8×10^{16} atoms $\cdot$ cm$^{-2} \cdot$ s^{-1}. The pressure of atomic oxygen is 0.01 Pa calculated by the Hertz–Knudsen equation from the flux density.

B. Silver Filament Sensor

A schematic representation of the silver filament sensor is depicted in Fig. 1. This sensor was used to study the kinetics of silver oxidation in atomic oxygen at different temperatures to reveal the temperature range of silver oxide formation. The kinetics of silver oxidation was studied by measuring electrical resistance evolution of a silver filament (diameter 0.5 mm) exposed to atomic oxygen fluxes. The filament was heated resistively, and the resistance was measured as a ratio of voltage drop on the central (evenly heated) part of the wire to electrical current through the filament. The electrical-resistance data were normalized by the initial resistance before oxidation (R/R_0) to avoid uncertainty in the distance between the potential contacts. The electrical conductivity of silver oxide formed on the specimen surface is negligible compared to that of silver metal; therefore a simple equation can be used to calculate the thickness of the formed oxide film from the resistance data:

$$h = \frac{h_0 \rho_{Ag} M_{Ag_2O}}{2\rho_{Ag_2O} M_{Ag}} \times \left(1 - \sqrt{\frac{1}{R/R_0}}\right) \tag{3}$$

where h is the thickness of the oxide layer (mm), h_0 is the initial diameter of the silver filament (mm), ρ_{Ag} and ρ_{Ag_2O} are the densities of silver and silver oxide (g $\cdot$ cm^{-3}), M_{Ag} and M_{Ag_2O} are the respective molecular weights, and R/R_0 is the electrical resistance of the specimen normalized by the initial value.

The experiments were repeated at least three times on different samples for the same conditions to achieve reproducibility of results. Oxide films formed on silver were analyzed by x-ray diffraction.

C. Nernstian Oxygen Sensor

Figure 2 depicts a schematic representation of a Nernstian-type sensor with a zirconia electrolyte for detection of atomic oxygen. The sensor was introduced into the vacuum chamber and heated with an electric oven. The temperature of the cell was measured by a K-type thermocouple. A voltmeter with high-ohmic input was used to measure EMF of the sensor. The sensor is based on a solid electrolyte (stabilized zirconia) tube with metallic electrodes. The

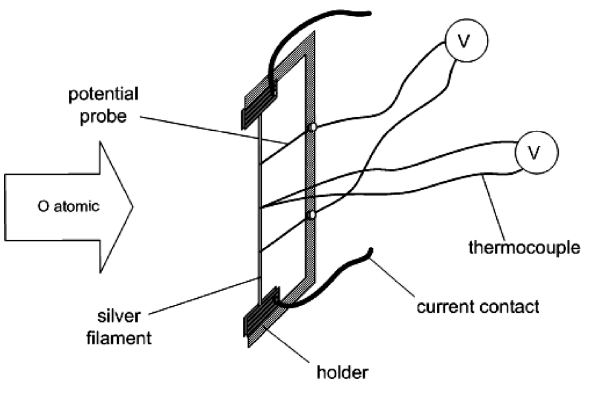

Fig. 1 Silver filament sensor for detecting atomic oxygen and study of silver oxidation kinetics.

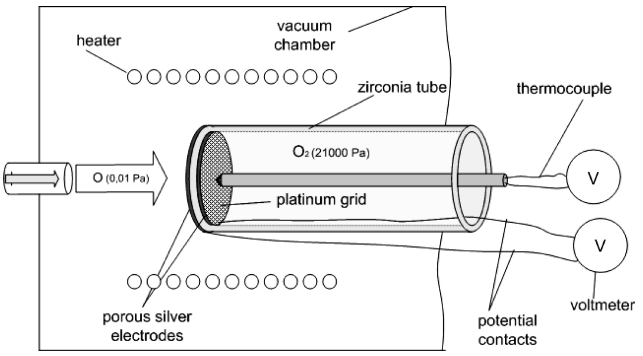

Fig. 2 Schematic representation of Nernstian oxygen sensor with zirconia electrolyte.

porous silver working electrode is deposited on the external side of the zirconia tube, which is exposed to fluxes of oxygen atoms. The internal part of the tube with attached platinum grid is in contact with atmospheric air and works as a reference electrode.

III. Scientific Idea

The chemical potential of atomic oxygen is higher than that for molecular oxygen, because the reaction of oxygen dissociation consumes energy to break down the chemical bond between two oxygen atoms:

$$O_2 \rightarrow 2O,\ \Delta_r G^0_{diss} = 464\ \text{kJ} \cdot \text{mol}^{-1} \tag{4}$$

The excess chemical potential of atomic oxygen can be transformed into chemical, mechanical, or electrical energy.[14]

Atomic oxygen is a more powerful oxidative agent than molecular oxygen due to enhanced chemical potential. For example, silver can be oxidized quickly by atomic oxygen; however, no oxidation occurs in the case of molecular oxygen. Earlier experiments showed that Ag_2O is formed on the silver surface in atomic oxygen environments.[6,9] Thermodynamic analysis shows that the reaction of silver oxidation (5) as well as dissociation of the formed silver oxide (6) is possible but depends on the temperature range:

$$2Ag + O \rightarrow Ag_2O \tag{5}$$

$$Ag_2O \rightarrow 2Ag + \tfrac{1}{2}O_2 \tag{6}$$

Gibbs energy of reactions (5) and (6) can be calculated from the standard enthalpies and entropies[15] using Eqs. (7) and (8).

Oxidation of silver by atomic oxygen:

$$\Delta_r G = \Delta_r H^0 - T\,\Delta_r S^0 - RT\,\ell n\,P_O \tag{7}$$

Dissociation of the silver oxide:

$$\Delta_r G = \Delta_r H^0 - T\,\Delta_r S^0 + (RT/2)\,\ell n\,P_{O_2} \tag{8}$$

where $\Delta_r G$ is Gibbs energy, $\Delta_r H^0$ is enthalpy, $\Delta_r S^0$ is entropy, R represents the universal gas constant, and P_O and P_{O_2} are partial pressure of atomic and molecular oxygen, respectively. The Gibbs energy of reactions depends on metal temperature and on the pressure of atomic and molecular oxygen in the gas phase as shown by Eqs. (7) and (8). Figure 3 presents the temperature dependencies of the Gibbs energy for reactions (5) and (6) at pressures of molecular and atomic oxygen of about 1.5×10^{-2} and 1.0×10^{-2} Pa, respectively. The reaction of Ag_2O formation (5) is thermodynamically possible at temperatures up to 1100 K. The opposite reaction of oxide dissociation (6) is also thermodynamically possible in this temperature range. However, the thermodynamic probability of oxidation is higher than that of the dissociation reaction up to 800 K, because the Gibbs energy is more negative for (5) in this temperature range. At temperatures higher than 800 K, the thermodynamic probability of oxide dissociation is higher than of the oxidation process. This means that increased temperature can stop the reaction of silver

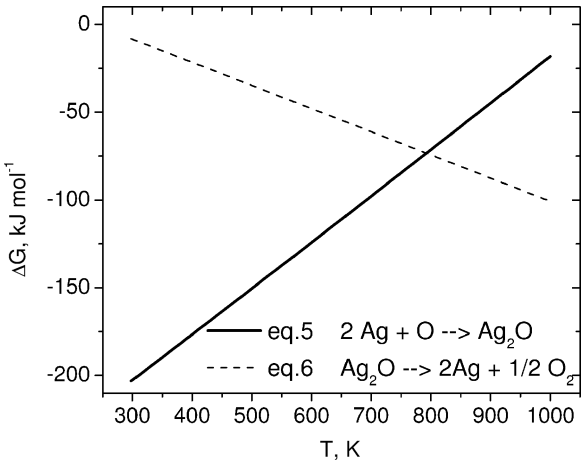

Fig. 3 Gibbs energy for oxidation reaction (5) and oxide dissociation reaction (6) as a function of temperature.

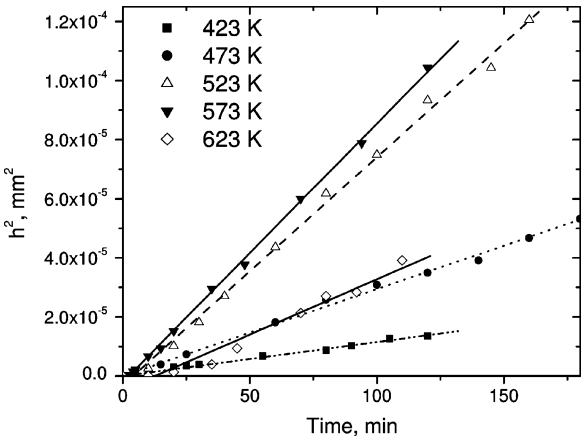

Fig. 4 Square of oxide film thickness as a function of oxidation time at the atomic oxygen incident flux of 2.7×10^{16} at $\cdot$ cm$^{-2} \cdot$ s^{-1} and different temperatures.

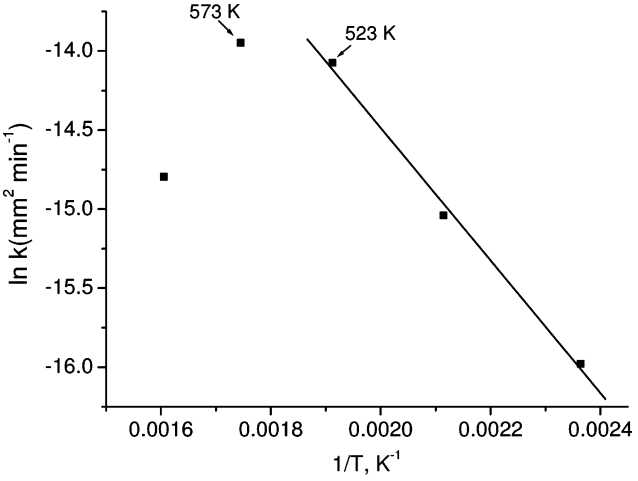

Fig. 5 Arrhenius plot of the parabolic rate constant for silver oxidation by atomic oxygen.

oxidation, which occurs at lower temperatures in an atmosphere of atomic oxygen. The temperature at which oxidation is stopped depends on the pressure of atomic oxygen, as shown in Eq. (7). Thus, the maximal temperature of silver oxidation in atomic oxygen is a single-valued characteristic of the pressure of the atomic gas.

The excess chemical potential of atomic oxygen can also be directly transformed to the EMF of a Nernstian-type galvanic cell with an oxygen-conducting solid electrolyte. As is well known, the EMF of such a cell depends on the difference of chemical potentials on opposite electrodes by the following equation:

$$\Delta E = \frac{\mu_{O_2} - \mu_O}{4F} = \frac{\Delta_r G_{diss}}{4F} + \frac{RT}{4F} \ell n \frac{P_O^2}{P_{O_2}} \qquad (9)$$

where μ_{O_2} and μ_O are chemical potentials of molecular and atomic oxygen, respectively. In an ideal case the EMF of such a cell depends only on the pressure of atomic oxygen and the temperature if the pressure of molecular oxygen is constant. Thus, the concentration of atomic oxygen can be sensed by measuring the EMF of a Nernstian sensor based on the developed galvanic cell.

IV. Results and Discussion

A. Oxidation-Based Sensor

The oxidation of silver in atomic oxygen (1.0×10^{-2} Pa) at temperatures between 423 and 700 K was investigated to confirm the thermodynamic interpretations presented in Sec. III. X-ray diffraction studies of the oxidized samples showed that Ag_2O was the only product of surface oxidation under the given conditions.

The oxidation rate in the temperature range from 423 to 623 K follows a parabolic law indicating the diffusion limitation of processes. Plots of the square of oxide thickness vs time are presented in Fig. 4.

Figure 5 presents the temperature dependence (Arrhenius plot) for the parabolic rate constant of silver oxidation. Oxidation rate increases according to the Arrhenius relation up to 523 K with activation energy 33 kJ $\cdot$ mol^{-1}. Further increase of temperature leads to slower growth of the oxidation rate. After that the parabolic constant achieves a maximum at about 573 K and then decreases. The oxidation kinetics changes from parabolic to linear when temperature reaches 648 K. The change of kinetic dependence shows that the oxidation mechanism has changed and the rate-limiting step is no longer diffusion but chemical reactions on the surface. The oxidation of silver by atomic oxygen stops when the temperature reaches 673 K. At this temperature, the oxide film formed at a lower temperature dissociates to molecular oxygen and silver metal, leading to decrease of the resistance of the previously oxidized filament. X-ray diffraction studies confirm that the surface oxide film disappears after such treatment.

This unusual temperature dependence can be explained in terms of the thermodynamic probability of the oxidation/dissociation processes described earlier. The rate of chemical processes is related to the thermodynamic probabilities (Gibbs energies) of reactions (5) and (6). However, this correlation is not definitive, because other important kinetic factors are involved, such as activation and diffusion barriers. At temperatures below 673 K the thermodynamic probability of the oxidation reaction (5) is higher than for the reaction of oxide dissociation (6); therefore oxidation (5) occurs faster than oxide dissociation (6). However, the thermodynamic probability of reaction (5) decreases with temperature, whereas that of reaction (6) increases. Around 773 K, the Gibbs energies of reactions (5) and (6) become equal, and at higher temperatures reaction (6) prevails. This temperature is reasonably close to 673 K, where oxidation stops, according to experiment, considering the relationship between thermodynamic and kinetic properties. At temperatures up to 673 K, silver oxide can be formed only as a thin film in local islands that have no effect on the resistance of the filament. Previously Dickens et al. found that oxidation of silver by atomic oxygen stops at 588 K (Ref. 16). This lower temperature value can be due to the lower pressure of atomic oxygen used, which changes the Gibbs energies of reactions (5) and (6) according to Eqs. (7) and (8).

Thus, the experimental results confirm that the silver cannot be oxidized by atomic oxygen at temperatures higher than T_{max}. The value of this maximal temperature (T_{max}) is related to the pressure of atomic oxygen. Therefore determination of the maximal temperature (T_{max}) at which silver oxidation is stopped can be used to measure the pressure (concentration) of atomic oxygen. The sensor for measurement of atomic oxygen concentration can be designed as a thin silver film to decrease energy consumption and increase sensitivity. Such a sensor is reusable and its response has no dependence

on the structure of the silver film, in contrast to actinometers used the kinetics of silver oxidation.[1,8,9]

B. Nernstian Sensor for Atomic Oxygen

The EMF of the Nernstian oxygen sensor (Fig. 2) was measured by exposing the silver porous electrode to the flows of molecular and dissociated oxygen at different temperatures. Partial pressures of molecular and atomic oxygen in the fluxes of dissociated gas were about 1.5×10^{-2} and 1.0×10^{-2} Pa, respectively. In the case of molecular gas flow, the oxygen pressure was about 2×10^{-2} Pa. The reference electrode was kept at atmospheric pressure during all experiments.

Figure 6 presents the temperature dependence of the sensor response (EMF). EMF of the sensor in molecular oxygen shows a linear dependence on temperature in the range from 770 to 1000 K. At lower temperatures, the sensor does not show a reproducible response to molecular oxygen due to slow processes of oxygen dissociation on the silver electrode at low temperatures. The EMF plot in atomic oxygen shows three different regions separated by two bends depending on operating temperature. In the first part, at 825–1000 K, the EMF of the sensor in atomic oxygen is about 100 mV higher than for the molecular gas. Further decrease of the temperature leads to significant increase of the EMF-vs-T slope (second part). The EMF of the cell achieves positive values at 700 K, indicating that the chemical potential of atomic oxygen (0.01 Pa) on the silver electrode is higher than the chemical potential of molecular oxygen (21,000 Pa) on the reference electrode. The slope of the temperature dependency decreases again in a third region at temperatures below 670 K. This behavior of the EMF plot will be discussed in terms of oxygen recombination on electrode surface.

Higher EMF values in atomic oxygen compared to the molecular gas can easily be explained in terms of enhanced chemical potential of atomic oxygen, as shown in Eq. (9). The calculated theoretical values of EMF under experimental conditions are also presented in Fig. 6. Theoretical EMF values in atomic oxygen are higher than experimentally measured response, because a significant part of the oxygen atoms recombine on the silver electrode, forming oxygen molecules. Thus, the effective chemical potential of atomic oxygen will be lower than the theoretical one. The additional coefficient α (electrode material, T) <1 depending on the electrode material and the temperature of the sensor should be introduced in this case into Eq. (9):

$$\Delta E = \frac{\mu_{O_2} - \mu_O}{4F} = \frac{\Delta_r G_{diss}}{4F} + \frac{RT}{4F} \ell_n \frac{(\alpha P_O)^2}{P_{O_2}} \qquad (10)$$

Part of the oxygen atoms recombine on the electrode surface at temperatures above 825 K, because the oxygen recombination coefficient on silver is very high. Thus, the difference in EMF values in molecular and atomic oxygen is relatively low in the first region of Fig. 6. The first islands of Ag_2O are formed on the electrode surface at temperatures below 800 K according to the thermodynamics of the oxidation/dissociation processes (Fig. 3). Formation of silver oxide film on metal surface leads to drastic decrease of the recombination coefficient, increasing the sensor response (second part in Fig. 6). The surface area of silver covered with oxide is increased with temperature decrease, leading to the higher slope of the EMF plot in the second temperature region. When the silver surface is completely covered with the oxide film ($T = 673$ K), the slope of temperature dependence decreases again (third region). However, the EMF values are higher in this region due to low recombination activity. The temperature at which silver surface is completely covered with oxide has the same value as T_{max} in the case of the silver oxidation experiments. This agreement between results of two different methods confirms once again the correctness of the interpretations.

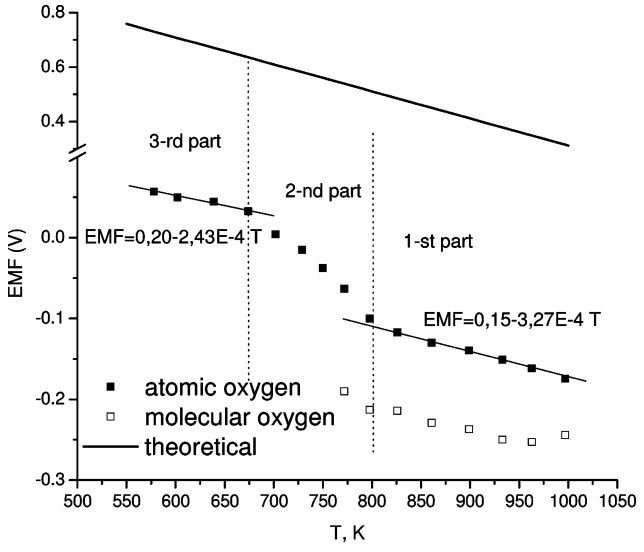

Fig. 6 EMF of the Nernstian sensor in atomic and molecular oxygen vs temperature.

The atomic oxygen concentration influences the EMF values and the shape of the EMF-vs-T curve, shifting positions of the bends according to Eq. (10). Thus, the precalibrated Nernstian cell can be used as a sensor for atomic oxygen, especially at lower temperatures, at which the oxygen atoms lead to higher response.

C. Design of New Complex Sensor

The two approaches presented can be used in one device designed as a complex sensor. A thin yttrium-stabilized zirconia (YSZ) plate can be used as a solid electrolyte and as a base for the sensor. The principal design of a similar sensor with platinum porous electrode for operation in molecular oxygen is described elsewhere.[17] A porous silver working electrode instead of a platinum one can be deposited on the exposed side of the plate (Fig. 7). The mixture of Ni/NiO applied on the counter side can work as a reference electrode. Thin metallic (silver) film deposition on the reference electrode is necessary to obtain a reliable electrical contact. The reference electrode should be also encircled by the oxygen diffusion barrier and protected by the glass layer. In addition to the described sensor, the thin silver strip can be deposited on the top side of the zirconia plate. This silver pathway can be used as a sensor for measurement of the maximal temperature of silver oxidation in atomic oxygen. The dielectric layer applied between the silver strip and zirconia plate can provide reliable electrical insulation.

Such a complex sensor can operate using the approaches described above. The sensor needs to be heated before exposure to the atomic oxygen atmosphere. Decrease of the sensor temperature leads to decreased resistance of the silver road. Silver oxidation starts at temperatures below T_{max}, influencing the temperature dependence of conductivity compared to that of the unoxidized silver pathway. The pressure of atomic oxygen can be then calculated from this maximal temperature (T_{max}) of silver oxidation as shown above. Additionally, the EMF of the Nernstian oxygen sensor can be measured. The complex signal from these two sensors can give a reliable estimate of atomic oxygen pressure in the gas phase after treatment by a programmed processor.

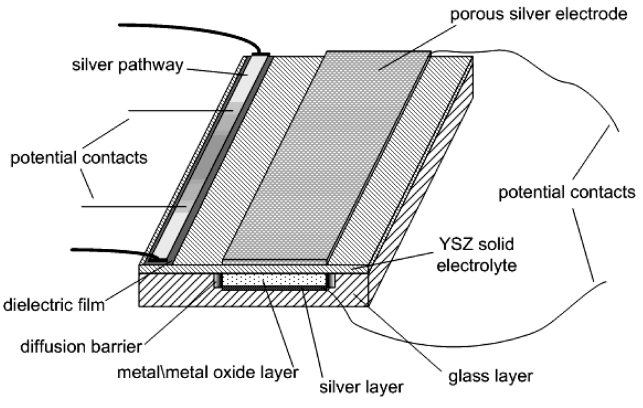

Fig. 7 Complex sensor for measurement of atomic oxygen pressure.

V. Conclusions

Two new thermodynamics-based approaches to atomic oxygen sensing are proposed in the present work. The methods are based on determination of the maximal temperature of silver oxidation and on measurement of EMF of a Nernstian oxygen sensor in an atmosphere of atomic oxygen.

The experimental results of the two methods are in good agreement with each other and with the proposed thermodynamical interpretations.

The design of a new complex sensor for atomic oxygen concentration measurement using both principles is proposed.

References

[1]Osborne, J. J., Harris, I. L., Roberts, G. T., and Chambers, A. R., "Satellite and Rocket-Borne Atomic Oxygen Sensor Techniques," *Review of Scientific Instruments*, Vol. 72, No. 11, 2001, pp. 4025–4041.

[2]Raja Reddy, M., "Effect of Low-Earth-Orbit Atomic Oxygen on Spacecraft Materials," *Journal of Materials Science*, Vol. 30, No. 2, 1995, pp. 281–307.

[3]Fujimoto, K., Shioya, T., and Satoh, K., "Degradation of Carbon-Based Materials due to Impact of High-Energy Atomic Oxygen," *International Journal of Impact Engineering*, Vol. 28, No. 1, 2003, pp. 1–11.

[4]Raspopov, S. A., Gusakov, A. G., Voropaev, A. G., Vecher, A. A., Zheludkevich, M. L., Lukyanchenko, O. A., Gritsovets, A. G., and Grishin, V. K., "Kinetics of Zirconium Oxidation by Atomic and Molecular Oxygen at Low Pressures," *Journal of the Chemical Society, Faraday Transactions*, Vol. 93, No. 11, 1997, pp. 2113–2116.

[5]Gusakov, A. G., Voropaev, A. G., Zheludkevich, M. L., Vecher, A. A., and Raspopov, S. A., "Studies of the Interaction of Copper with Atomic and Molecular Oxygen," *Physical Chemistry Chemical Physics*, Vol. 1, No. 23, 1999, pp. 5311–5314.

[6]Zheludkevich, M. L., Gusakov, A. G., Voropaev, A. G., Vecher, A. A., Kozyrski, E. N., and Raspopov, S. A., *Protection of Materials and Structures from Space Environment: Proceedings of ICPMSE-6, Sixth International Space Conference*, edited by J. I. Kleiman and Z. Iskanderova, Kluwer Academic, 2003, pp. 351–359.

[7]Zheludkevich, M. L., Gusakov, A. G., Voropaev, A. G., Vecher, A. A., Yasakau, K. A., and Ferreira, M. G. S., "Influence of Oxygen Dissociation on the Oxidation of Iron," *Oxidation of Metals*, Vol. 62, No. 3–4, 2004, pp. 223–235.

[8]Harris, I. L., Chambers, A. R., and Roberts, G. T., "Preliminary Results of an Atomic Oxygen Spaceflight Experiment," *Materials Letters*, Vol. 31, No. 3–6, 1997, pp. 321–328.

[9]Miller, G. P., Pettigrew, P. J, Raikar, G. N., and Gregory, J. C., "A Simple, Inexpensive, Hyperthermal Atomic Oxygen Sensor," *Review of Scientific Instruments*, Vol. 68, No. 9, 1997, pp. 3557–3562.

[10]Osborne, J. J., Roberts, G. T., Chambers, A. R., and Gabriel, S. B., "Initial Results from Ground-Based Testing of an Atomic Oxygen Sensor Designed for Use in Earth Orbit," *Review of Scientific Instruments*, Vol. 70, No. 5, 1999, pp. 2500–2506.

[11]Osborne, J. J., Roberts, G. T., Chambers, A. R., and Gabriel, S. B., "Thin-Film Semiconductor Sensors for Hyperthermal Oxygen Atoms," *Sensors and Actuators B*, Vol. 63, No. 1–2, 2000, pp. 55–62.

[12]Gutman, E. E., "Space and Aircraft Sensors," *Sensors and Actuators B*, Vol. 18, Nos. 1–3, 1994, pp. 22–27.

[13]Raspopov, S. A., Gusakov, A. G., Voropaev, A. G., Vecher, A. A., and Grishin, V. K., "Interaction of Tantalum with Diatomic and Atomic Oxygen at Low-Pressures," *Journal of Alloys and Compounds*, Vol. 201, No. 1–2, 1993, pp. 67–72.

[14]Vecher, A. A., Voropaev, A. G., Gusakov, A. G., Zheludkevich, M. L., and Savitsky, A. A., "Several Thermodynamical Aspects of Interaction of Atomic Gases with Materials," *Doklady Natsionalnoi Akademii Nauk Belarusi*, Vol. 46, No. 1, 2002, pp. 64–67.

[15]NIST Chemistry WebBook, URL: http://webbook.nist.gov/chemistry/ [cited 22 Jan. 2006].

[16]Dickens, P. G., Heckingbottom, R., and Linett, J. W., "Oxidation of Metals and Alloys Part 2. Oxidation of Metals by Atomic and Molecular Oxygen," *Transactions of the Faraday Society*, Vol. 65, 1969, pp. 2235–2246.

[17]van Setten, E., Gür, T. M., Blank, D. H. A., Bravman, J. C., and Beasley, M. R., "Miniature Nernstian Oxygen Sensor for Deposition and Growth Environments," *Review of Scientific Instruments*, Vol. 73, No. 1, 2002, pp. 156–161.

J. Kleiman
Guest Editor